Soluble Epoxide Hydrolase Deficiency Inhibits Dextran Sulfate Sodium-induced Colitis and Carcinogenesis in Mice

WANYING ZHANG[1*], HAONAN LI[1*], HUA DONG[2], JIE LIAO[1],
BRUCE D. HAMMOCK[2] and GUANG-YU YANG[1]

[1]Department of Pathology, Northwestern University, Feinberg School of Medicine, Chicago, IL, U.S.A.;
[2]Department of Entomology, University of California, Davis, CA, U.S.A.

Abstract. *Soluble epoxide hydrolase (sEH) hydrolyses/ inactivates anti-inflammatory epoxyeicosatrienoic acids (EETs) to their corresponding diols, and targeting sEH leads to strong anti-inflammatory effects. In the present study, using a tissue microarray and immunohistochemical approach, a significant increase of sEH expression was identified in ulcerative colitis (UC)-associated dysplasia and adenocarcinoma. The effects of deficiency in the sEH gene were determined on dextran sulfate sodium (DSS) colitis-induced carcinogenesis. The effects of EETs on lipopolysaccharide (LPS)-activated macrophages were analyzed in vitro. With extensive histopathological and immunohistochemical analyses, compared to wild-type mice, sEH$^{-/-}$ mice exhibited a significant decrease in tumor incidence (13/20 vs. 6/19, p<0.05) and a markedly reduced average tumor size (59.62±20.91 mm^3 vs. 22.42±11.22 mm^3), and a significant number of pre-cancerous dysplasia (3±1.18 vs. 2±0.83, p<0.01). The inflammatory activity, as measured by the extent/proportion of erosion/ulceration/dense lymphoplasmacytosis (called active colitis index) in the colon, was significantly lower in sEH$^{-/-}$ mice (44.7%±24.9% vs. 20.2%±16.2%, p<0.01). The quantitative polymerase chain reaction (qPCR) assays demonstrated significantly low levels of cytokines/chemokines including monocyte chemoattractant protein (MCP-1), inducible nitric oxide synthase (iNOS), vasopressin-activated calcium-mobilizing (VCAM-1), interleukin-1 beta (IL-1β) and tumor necrosis factor-alpha (TNF-α). In vitro, LPS-activated macrophages treated with 14,15-EET showed a significant reduction of LPS-triggered IL-1β and TNF-α expression. Eicosanoic acid metabolic profiling revealed a significant increase of the ratios of EETs/ dihydroeicosatrienoic acids (DHETs) and epoxyoctadecennoic acid/dihydroxyoctadecenoic acid (EpOMEs/DiHOMEs). These results indicate that sEH plays an important role in the development of colitis and in inducing carcinogenesis.*

*These Authors contributed equally to this work.

Correspondence to: Guang-Yu Yang, MD, Ph.D., Northwestern University, Feinberg School of Medicine 303 E. Chicago Avenue, Chicago, IL 60611, U.S.A. Tel: +1 3125030645, Fax: +1 3125030647, e-mail: g-yang@northwestern.edu or Jie Liao, MD, Northwestern University, Feinberg School of Medicine 303 E. Chicago Avenue, Chicago, IL 60611, U.S.A. Tel: +1 3125031260, Fax: +1 3125030647, e-mail: jie-liao@northwestern.edu

Key Words: Soluble epoxide hydrolase, dextran sulfate sodium, colitis, carcinogenesis, mice.

Chronic inflammation is a well-recognized risk factor that plays a crucial role in initiating and promoting the development of many types of cancers (1, 2). A typical example is inflammatory bowel disease (IBD) that comes with a markedly increased risk of colorectal cancer (CRC) (3-5). IBD is an idiopathic, longstanding, chronic active inflammatory process in the gut and includes two diseases: ulcerative colitis (UC) and Crohn's disease. The incidence of CRC has been increasing in patients with UC and the risk of CRC increases with increased extent and duration of UC. In population-based cohorts, UC increases the risk of CRC by 2.4-fold (6). Crohn's disease presents similar epidemiological findings regarding its risk of cancer development. Several pro-inflammatory mediators are involved in inflammation and carcinoma development; arachidonic acid metabolites, such as prostaglandins and leucotrienes, are inflammatory instigators playing a crucial role in this process.

Prostaglandins and leucotrienes are generated from arachidonic acid mediated by the enzymes cyclooxgenase and lipoxygenase (7, 8). Epoxyeicosatrienoic acids (EETs) are products of arachidonic acid metabolism mediated by cytochrome *P450* which display an anti-inflammatory action (9). Under physiological conditions, soluble epoxide hydrolase (sEH) catalyzes the conversion of EETs to their corresponding dihydroxyeicosatrienoic acids (DHETs) (10, 11), and abolishes their anti-inflammatory effects (9). Inhibition or gene knockout of sEH stabilizes EETs and increases the EET-to-DHET ratio, leading to inhibition of inflammation through suppression of nuclear factor kappa-B

(NF-κB) activity and tumor necrosis factor (TNF-α)-induced expression of vascular cell adhesion molecules such as VCAM-1 (12, 13). Our previous study using a spontaneous colitis model in interleukin-10 (IL-10)-knockout mice demonstrated that sEH deficiency significantly reduces inflammatory activity and carcinoma development in the bowel (11, 14). Mechanistic study is highly parallel to the down-regulation of cytokines and chemokines TNF-α, monocyte chemoattractant protein-1 (MCP1), and IL-12, -17 and -23 and NF-κB signals in sEH-deficient mice, as well as the increased ratio of EET-to-DHET and EpOME-to-DiHOME. Whether or not these anti-inflammatory effects of *sEH* gene deficiency or inhibition extend to other inflammatory models needs to be investigated further.

Dextran sulfate sodium (DSS)-induced colonic active inflammation highly mimics human UC both clinically and histopathologically (7, 15-17). A sequence of DSS-induced colitis-dysplasia-carcinoma in long-term experimental settings is a typical model for studying IBD and cancer (18-23). This model has been extensively used to study cytokines and chemokines involved in IBD, as well as chemopreventive compounds such as inositol (19, 22-24). In the present study, the expression of sEH in human UC, UC-associated dysplasia and colorectal carcinomas was analyzed immunohistochemically using a tissue array approach. The effects of *sEH* gene deficiency in long-term DSS-induced UC and carcinogenesis were determined in mice with *sEH* gene-knockout. Development of tumors and dysplasia in the colon was analyzed both histopathologically and immunohistochemically. Inflammatory activities, cytokines, and chemokines were analyzed immunohistochemically as well as using a qPCR approach. Effects on the expression of key inflammatory cytokines in *in vitro*-cultured macrophages treated with LPS and EETs were analyzed using a qPCR approach. The eicosanoid metabolic profile was analyzed using a liquid chromatographic/mass spectrometric (LC/MS-MS) method.

Materials and Methods

Reagents. Reagents and antibodies used in this study were: Dextran sulfate sodium salt (MP Biomedicals, LLC, Solon, OH, USA), AIN93M/2XFe diet (Research Diets, Inc., New Brunswick, NJ, USA), antibodies against myeloperoxidase (rabbit pAb; Abcam, Cambridge, MA, USA), anti-Ki67 (rabbit mAb; Vector Laboratories Inc., Burlingame, CA, USA), and sEH (rabbit pAb, Santa Cruz Biotechnology, Inc., Santa Cruz, CA, USA), biotinyted anti-rabbit IgG secondary antibody and avidin/biotinylated enzyme complex (ABC, peroxidase system, Vector Laboratories Inc., Burlingame, CA, USA), diaminobenzidine, LPS and Mayer's hemotoxylin (Sigma-Aldrich, St.Louis, MO, USA), RPMI-1640 medium (Cellgro, Mannasa, VA, USA), 14,15-epoxy-*eicosatrienoic* acid (Cayman Chemical Company, Ann Arbor, MI, USA), RNeasy Kit (Qiagen, Inc., Valencia, CA, USA), SuperScript III Platinum Two-Step qRT-PCR Kit with SYBR Green (Invitrogen, Carlsbad, CA, USA), and diethyl procarbonate (EMD Chemicals, Gibbstown, NJ, USA). All the primers for PCR assays were purchased from Integrated DNA Technologies, San Jose, CA, USA.

Animal experiments. The Institutional Animal Care and Use Committee at Northwestern University approved all animal experiments (NU2011-1389). C57BL/6J mice were purchased from Jackson Laboratory (Bar Harbor, ME, USA), and sEH−/− mice in a C57BL/6J background were provided by Dr. Hammock, the University of California, Davis, CA (25). All mice were housed in micro-isolator cages (3-5 mice/cage) in a room illuminated with 12 h/12 h light-dark cycle and with free access to water and chow in the animal facilities at the Center for Comparative Medicine at Northwestern University.

Four groups of animals were enrolled at the beginning of the experiments: Wild-type and sEH−/− mice as negative controls (n=5 mice/group), and wild-type and sEH−/− mice treated with DSS (n=20 mice/group). DSS was administered to mice in the drinking fluid throughout the experiment. According to our previously-established methods (20), mice were subjected to 12 consecutive DSS cycle treatments; each cycle was defined as 1% DSS (w/v in de-ionized water) given to mice through the drinking fluid for seven days, followed by 10 days of ordinary tap water that allowed mice to recover from DSS-induced active inflammation in the colon. The cyclic protocol of DSS treatment mimics clinical flare-up and flare-down inflammatory activity in ulcerative colitis (22). All mice were fed with AIN93M diet containing 90 mg iron per kg diet. The mice were sacrificed at the end of the 12th DSS cycle (for a total treatment of 204 days).

Specimen collection and tissue processing. Mice sacrificed before the completion of 12 DSS cycles due to significant weight loss (>20%), excessive rectal bleeding and loss of activity were excluded from the results of the carcinogenesis experiment.

Mice were sacrificed by CO_2 asphyxiation. Blood and plasma were collected *via* heart puncture and stored in a freezer at −80°C until analysis. All key organs were collected. Briefly, the colon was inflated by *in situ* intra-luminal perfusion with chilled normal saline solution and opened longitudinally. The number, size and distribution of ulcers and tumors were measured and recorded. Tumor volume was calculated using the equation $V=4/3\pi r^3$, where r was the average tumor radius obtained from the two diameter measurements. Mucosal tissue from half of the colon was collected freshly in RNALater (Qiagen, Inc. Toronto, Canada) for RNA extraction for qPCR assay. The other half of the colon was fixed in 10%-buffered formalin, prepared as "swiss rolls", and processed for paraffin sections for histopathological and immunohistochemical analyses.

Histopathological analysis. According to our previously-established criteria (20-22), colorectal tumor, dysplasia and inflammatory activity were analyzed histopathologically. The carcinomas were further classified as polypoid adenocarcinomas with well, moderate, or poorly differentiated pattern (based on formation of glandular structure), and mucinous carcinomas (based on mucin production in more than 50% of the tumor). Dysplasia was characterized by partial loss of cell polarity and maturation, nuclear atypia, and an increase in mitotic figures. The grading of colonic inflammatory activity was mainly measured by the extent/proportion of inflammatory erosion/ulceration and intense lymphoplasmacytosis (analyzed for the density of lymphoplasma cells in the inflamed mucosa) in the colon, and the percentage of myeloperoxidase-stained neutrophils in the total cells counted in the inflamed colonic mucosa.

Immunohistochemistry. Immunohistochemical staining was performed using avidin/biotinylated enzyme complex-ABC peroxidase system on paraffin embedded tissue sections as previously described (11).

Human ulcerative colitis-UC tissue microarrays were established with 180 tissue specimens including 72 UC, 54 dysplasias, and 54 adenocarcinomas, with each specimen having four tissues cores obtained from achieved tissues of Northwestern Memorial Hospital (with approval of institutional IRB # STU00047832). The primary antibodies included antibodies against myeloperoxidase, Ki67, and sEH. Biotinyted anti-rabbit IgG secondary antibody was purchased from Vector Laboratories Inc. Diaminobenzidine was used as the chromogen. Slides were washed three times with TBST buffer between incubations and counterstained with Mayer's hemotoxilin for 1 min. sEH expression was analyzed based on the staining intensity, and graded as 0: no staining or background staining, 1: faint or weak staining intensity and 2: intense staining. The number of myeloperoxidase-labeled neutrophils, and Ki-67-labeled proliferative cells per high power (×40 objective lens) were counted to determine the percentage of positive cells out of the total cells counted.

Peritoneal macrophage isolation and cell culture. Five C57BL/6J mice were sacrificed. A 30% sucrose solution (10 ml per mouse) was injected into the peritoneal cavity, gently palpated for about 5 min, and then the fluid was aspirated out. Collected fluid was spun down and washed with RPMI-1640 medium containing 10% fetal bovine serum (FBS) and 500 µl gentamicin (complete medium). Cells (3×10^6/3 ml/well) were seeded in 6-well dishes with the complete medium for 2 h at 37°C in 5% CO_2 in a humidified incubator, and then were replenished with fresh medium to remove erythrocytes and floating cells. The attached cells defined as macrophages were cultured for 24 h, followed by treatment with LPS at a dose of 10 µg/ml and 14,15-EET at the doses of 500 nM and 1 µM for 24 h. Cells were then washed with cold PBS, trypsinized, and harvested by centrifugation. Total RNA was extracted for quantitative analysis of inflammatory cytokines using a real time RT-PCR assay.

Quantitative real-time PCR. Total RNA was extracted from the colonic mucosa and cultured macrophages using the RNeasy Kit (Qiagen, Inc.), and the concentration was measured using a SmartSpec Plus Spectrophotometer (BioRad, Hercules, CA, USA). cDNA was synthesized using 1 µg of total RNA in a 20 µl reverse transcriptase reaction mixture using SuperScript III Platinum Two Step qRT-PCR Kit with SYBR Green (Invitrogen) according to the manufacturer's instructions. The detailed methods were described in our previous publication (11). All real-time RT-PCR reactions were performed in a 20 µl mixture containing 1/10 volume of cDNA preparation (2 µl), 10 µl SYBR Green buffer, 0.4 µM of each primer, 6.8 µl diethylprocarbonate (EMD Chemicals). Real-time PCR for mRNA quantification was performed using the MiniOpticon Real Time PCR System (Bio-Rad). PCR conditions were: 50°C for 2 min, 95°C for 2 min, followed by 40 cycles of 95°C, 15 s; 58°C, 3 s; 50°C, 1 s. Data for each mRNA expression experimental are shown as the relative fold-change normalized by that of glyceradehyde-3-phosphate dehydrogenase (GAPDH).

Analysis of arachidonic acid metabolic profile using LC/MS-MS method. LC/MS-MS analysis of oxylipids was performed using a modified method. The detailed methods for sample treatments and analysis were described in our previous publication (11, 14).

Statistical analysis. Each analyzed parameter is expressed as the mean±SD, unless otherwise stated, with at least three independent measurements. Continuous variables were compared with the Student's *t*-test, whereas categorical variables were compared with Chi-square test. All statistical tests were two-tailed; statistical significance was set at $p<0.05$.

Results

Expression of sEH in human UC and UC-associated dysplasia and adenocarcinoma. In order to determine the status of sEH expressed in human UC and its associated dysplasia and adenocarcinoma, tissue microarrays were established, which included 180 patients in total with UC (72 patients), dysplasia (54 patients), and adenocarcinoma (54 patients), each specimen with four tissue cores in the array. Using a specific antibody against sEH through an immunohistochemical approach, distinct expressions of sEH in these microarray samples were detected. Our results showed that non-neoplastic colonic epithelia displayed weak positivity in 39% (n=72, 28/72) of cases, mainly expressing focal epithelia with reactive hyperplastic changes (Figure 1A); while 88.9% (n=54, 48/54) of UC-associated dysplasia (Figure 1B) and 94% (n=54, 51/54) of UC-associated adenocarcinoma displayed positivity (Figure 1C). Further semi-quantification of the staining intensity showed a significant ($p<0.05$) increase of sEH expression in UC-associated dysplasia and adenocarcinoma (Figure 1D).

sEH Gene deficiency inhibited DSS-induced colitis-associated carcinogenesis in mice. Body weight, food and water consumption were carefully monitored during the animal experiment. There was no difference in the average body weight, food and water consumption between the sEH$^{-/-}$ mice and wild-type mice treated with or without DSS (data not shown). The average body weight of sEH$^{-/-}$ mice did not differ from that of wild-type C57/6j mice at the end of the experiment (average body weights 24.34±3.0 g in sEH$^{-/-}$ mice *vs*. 24.49±2.9 g in C57/6j mice, $p>0.05$).

Tumor development was analyzed both grossly and histopathologically. No tumor was seen in wild-type nor sEH$^{-/-}$ mice without DSS treatment. A significant reduction of colorectal carcinoma development was observed in sEH$^{-/-}$ mice with DSS-induced colitis ($p<0.05$) (Figure 2G and H). Histopathological analysis showed that the majority of colonic tumors were well-differentiated mucinous carcinomas with invasion into the muscularis propria or subserosa (Figure 2A-C). Mucinous carcinoma incidence was greater in wild-type mice than in sEH$^{-/-}$ mice (9/20 *vs*. 3/20) but the difference did not reach statistical significance ($p>0.05$). Polypoid adenocarcinomas, characterized by well-differentiated glandular/tubular growth pattern with invasion into the *lamina propria* or submucosa (Figure 2D), were identified in 5/20 of the wild-type mice, while no polypoid adenocarcinomas were found in sEH$^{-/-}$ mice ($p<0.01$).
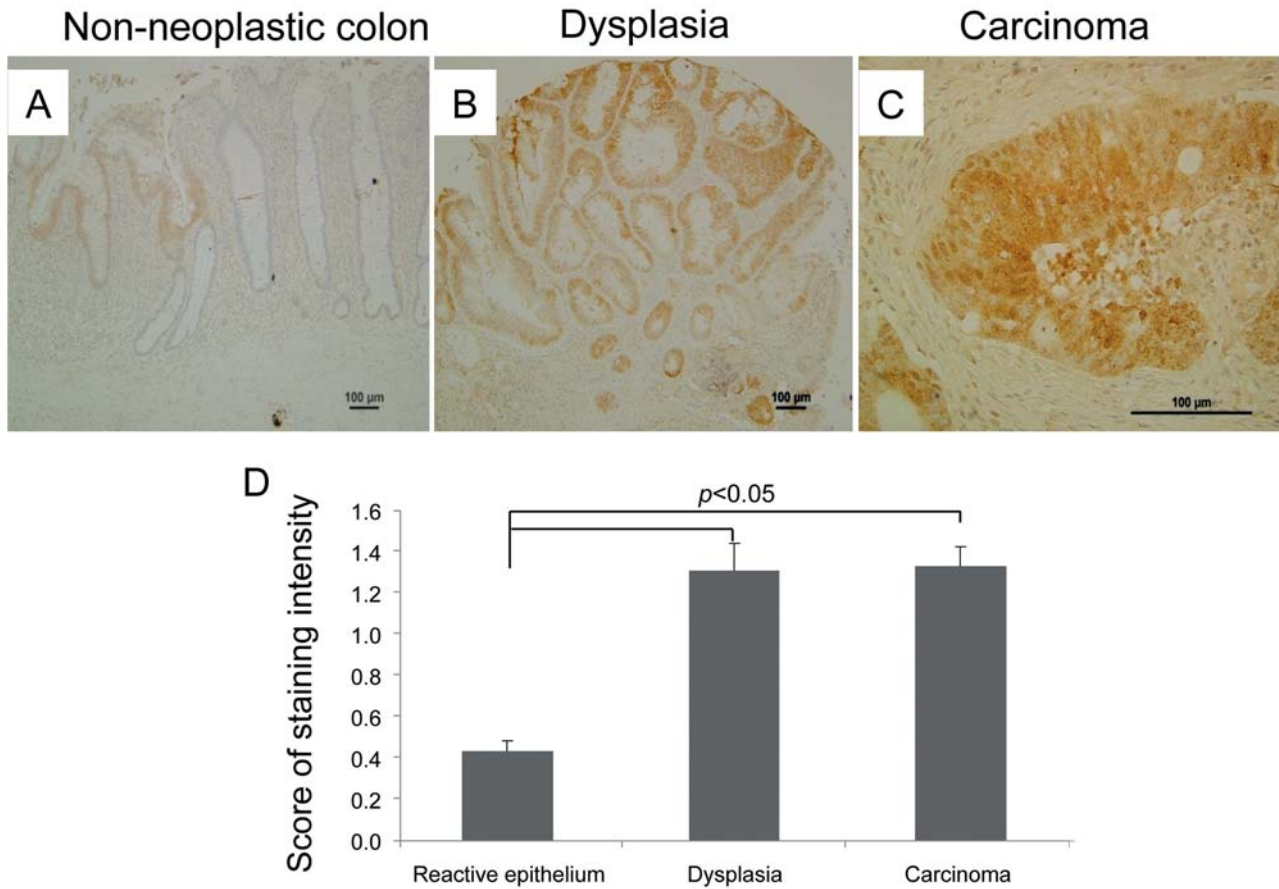
Figure 1. *Immunohistochemical analysis of soluble epoxide hydrolase (sEH) expression in human ulcerative colitis (UC) and its associated dysplasia and adenocarcinoma. A: Non-neoplastic colonic mucosa showing focal reactive/hyperplastic epithelium with positive sEH staining; B: UC-associated dysplasia with intense sEH staining; C: UC-associated adenocarcinoma with intense sEH staining; D: Histogram of semi-quantification of sEH staining intensity. Compared to the non-neoplastic colonic mucosa, the intensity of sEH staining in both dysplasia and carcinoma was significantly increased (p<0.05).*

IBD-induced dysplasia in the colon was analyzed histopathologically and immunochemically. Morphologically, dysplasia is characterized as the partial loss of nuclear polarity and cell maturation, with nuclear atypia and an increased mitotic activity (Figure 3D). All wild-type mice with DSS-induced colitis carried colonic dysplastic lesions, with an average 3 ± 1.18/mouse, while 18/20 of sEH$^{-/-}$ mice with DSS-induced colitis carried on average 2 ± 0.83 colonic dysplastic lesions per mouse ($p<0.01$, Figure 3D). Proliferation as determined by Ki-67 labeling was crucial for characterizing dysplastic lesions. In inflamed colonic mucosa, Ki-67-labeling proliferative cells were predominantly located in the crypt compartment (Figure 3A), while in the dysplastic lesions, Ki-67-labeled proliferative cells were observed in both crypt epithelium and upper/superficial compartments (Figure 3B). Semi-quantitative analysis of Ki-67-labeled cell proliferative cells was performed for both the superficial-differentiated and the deep-crypt proliferation compartments in colonic mucosa. A significant decrease of Ki-

67-labeled cells in the upper/superficial compartments of mucosa in the inflamed mucosa ($p<0.01$) and in the dysplastic lesions ($p<0.01$) was observed in sEH$^{-/-}$ mice compared to wild-type mice (Figure 3C), but there was no statistical difference in Ki-67-labeled cell proliferation in the deep-crypt proliferation compartment in colonic mucosa.

Histopathological and immunohistochemical analyses of colonic inflammatory activity. Morphologically, inflammatory activity was analyzed based on the extent of inflammation (proportion of the colonic mucosa with erosion/ulcerative/lymphoplasmacytosis in the total colonic mucosa) or defined as the percentage of inflamed area in the colon (Figure 4A and B). The percentage of inflamed area in the colon was significantly greater in wild-type than in sEH$^{-/-}$ mice ($44.7\%\pm24.9\%$ *vs.* $20.2\%\pm16.2\%$, $p<0.01$). In addition, more wild-type mice had more than 50% inflammation or active colitis in the colon compared to the sEH$^{-/-}$ ($p<0.05$) (Figure 4C).
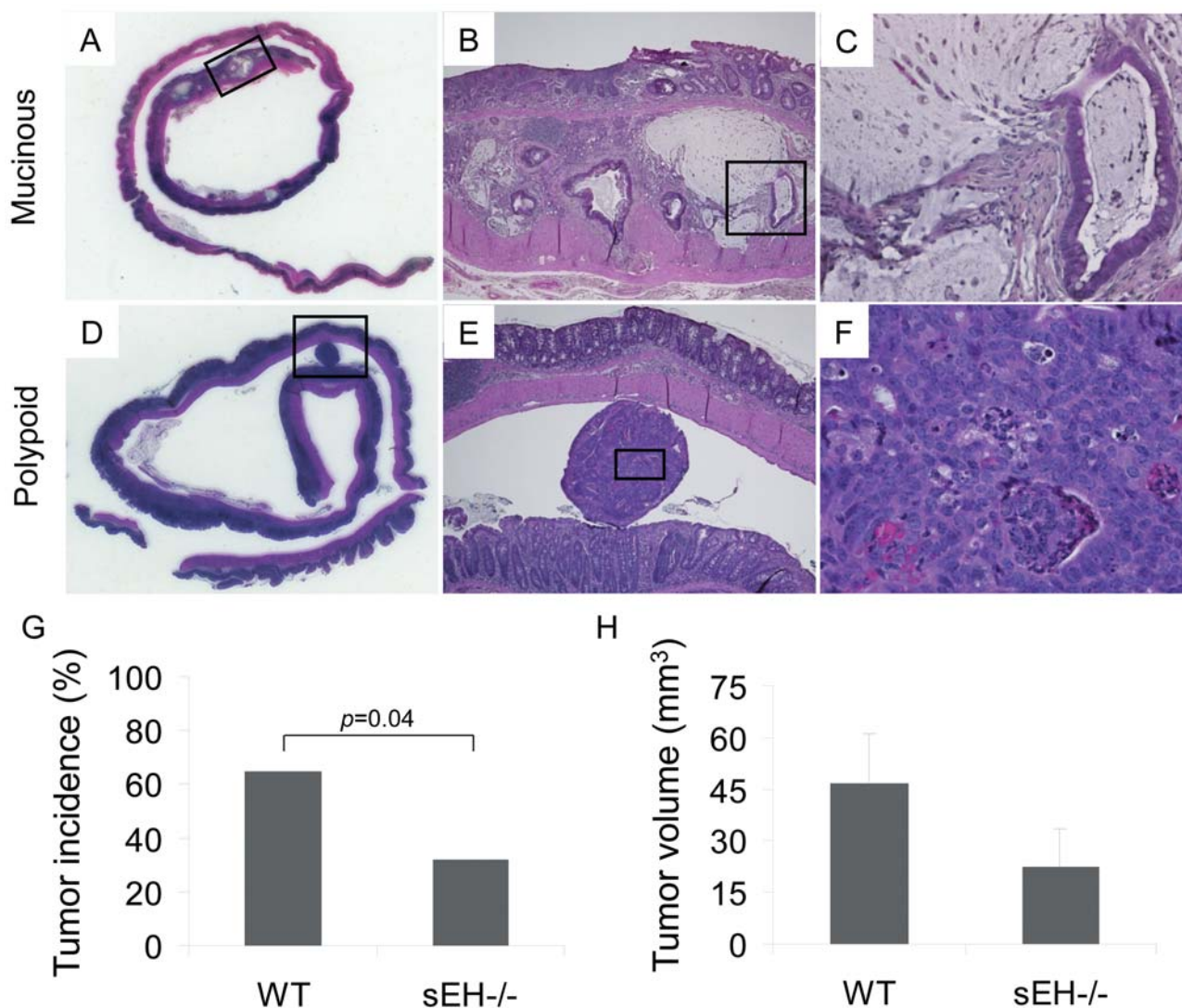
Figure 2. *Histopathological analysis of colorectal carcinoma in dextran sulfate sodium (DSS)-induced colitis in both wild-type and sEH$^{-/-}$ mice. A-C: Representative photographs of invasive mucinous adenocarcinoma (from low ×20 to high ×400 magnification); D-F: Representative pictures of polypoid well differentiated adenocarcinoma (from low ×20 to high ×400 magnification); G: Histogram of tumor incidence; H: Histogram of average tumor volume. Results are expressed as the mean±SD.*

Active inflammatory cells or neutrophils labeled by myeloperoxidase (MPO) immunostaining were further analyzed immunohistochemically. The number of MPO-labeled neutrophils was counted and expressed as percentage of total cells counted. Compared to wild-type mice, significantly fewer MPO-labeled neutrophils were observed in sEH$^{-/-}$ mice ($p<0.05$) (Figure 4F).

Analysis of key inflammatory cytokines and chemokines in the cultured LPS-activated macrophages treated with 14,15-EET and in the colonic mucosal tissues. Transcriptional expression of IL-1β and TNF-α in LPS-activated macrophages with and without 14,15-EET treatment were quantitatively analyzed using the qPCR assay. As seen in Figure 5A and B, significant increases of both IL-1β and TNF-α expression were observed in LPS-activated macrophages compared to vehicle-treated cells, while a significant reduction of mRNA expression of IL-1β and TNF-α were observed in 14,15-EET-treated cells ($p<0.01$). Transcriptional expression of inflammatory cytokines and chemokines were further analyzed in freshly-collected colonic mucosa (n=6 mice/group). Wild-type and sEH$^{-/-}$ mice without DSS treatment led minimal expressions of MCP-1, iNOS, VCAM-1, IL-1β, TNF-α, and IFN-γ. By setting the value of each

Figure 3. *Quantitative analysis of Ki-67-labeled proliferative cells in the superficial and crypt compartments of colonic epithelium in dextran sulfate sodium (DSS)-induced colitis. A: Active colitis in both wild-type (WT, left) and sEH^{−/−} mice (right); B: Colitis-induced dysplasia in both WT (left) and sEH^{−/−} mice (right); C: Histogram showed a significant reduction of Ki-67-labeled proliferative cells (percentage of the Ki-67-labeled proliferative cells) within the superficial compartment in both of active colitis and dysplasia in sEH^{−/−} mice compared to WT mice (p<0.01). D: Histogram showed that the number of dysplastic lesions in DSS-induced colitis was significantly reduced in sEH^{−/−} mice compared to WT mice (p<0.01). The results are expressed as the mean±SD.*

cytokine expression in wild-type mice as 1, significant decreases of MCP-1, iNOS, VCAM-1, and IL-1β were found in sEH^{−/−} ($p<0.01$). The expression of TNF-α and IFN-γ were markedly decreased in sEH^{−/−} mice, but did not reach statistical significance ($p>0.05$, Figure 5C and D).

Plasma eicosanoid profile using LC/MS-MS. The ratio of fatty acid epoxides (EpOMEs) to their corresponding diols (DiHOMEs), as well as EETs to DHETs, are the most crucial biomarkers for determining sEH activity *in vivo*. Using LC/MS-MS, plasma levels of EETs, including 11(12)-EET, 14(15)-EET,
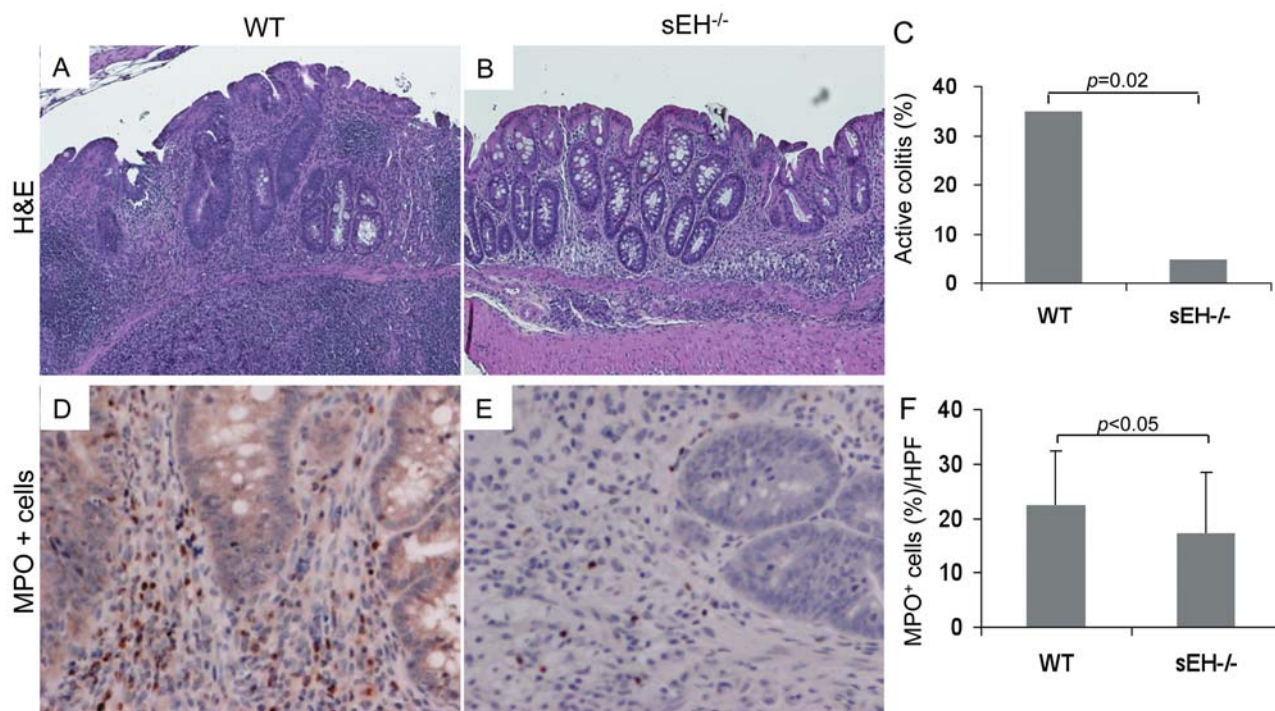
Figure 4. *Histopathological and immunohistochemical analysis of dextran sulfate sodium (DSS)-induced colitis. A: Colonic mucosa showing focal mucosal erosion and intense lymphoplasmocytosis in wild-type (WT) mice; B: Much less intense lymphoplasmocytosis within the lamina propria of the colonic mucosa in sEH$^{-/-}$ mice; C: Histogram of semi-quantification of active colitis (the percentage of inflamed area in the colon) showing a significant decrease of active colitis in sEH$^{-/-}$ mice compared to WT mice (p<0.05). Myeloperoxidase (MPO)-labeled neutrophils in active colitis in WT mice (D) and sEH$^{-/-}$ mice (E). F: Histogram of percentage of MPO-labeled neutrophils out of total cells counted showing a significant decrease of MPO-labeled neutrophils in sEH$^{-/-}$ mice compared to WT mice (p<0.05).*

and the fatty acid epoxides (EpOME), including 9(10)-EpOME and 12(13)-EpOME, as well as their corresponding diols, were quantitatively analyzed. The ratios of EET/DHET and EpOME/DiHOME (sum of all EETs and DHETs, and EpOMEs and DiHOMEs) were significantly increased in sEH$^{-/-}$ mice, compared to wild-type mice (Figure 6).

To investigate whether there was an effect of *sEH* gene-deficiency on modulating the other metabolic pathways of arachidonic acid, including cyclooxygenase (COX2) and lipoxygenase (LOX)-mediated metabolites, all of these metabolites, including prostaglandin E_2 (PGE$_2$), PGD$_2$, thromboxane B_2 (TXB$_2$), leukotriene B_4 (LTB$_4$) and 5-hydroxyeicosatetraenoic acid (5-HETE) were analyzed. Our results showed that there were no significant difference in their levels between wild type mice and sEH$^{-/-}$ mice.

Discussion

sEH converts anti-inflammatory EETs to their corresponding diols and leads to the inactivation of their physiological function. sEH protein is distributed in different human organs and tissues (26). Its intracellular localization is cell-specific; sEH is both cytosolic and peroxisomal in human hepatocytes and renal proximal tubules, but exclusively cytosolic in other sEH-containing cells such as intestinal epithelium (26). It has been demonstrated that sEH expression in cancer is tumor type-dependent. In renal and hepatic tumors, sEH was down-regulated, but in seminoma, cholangiocarcinoma and advanced ovarian cancer, the expression of sEH was up-regulated (27-29). Our study with resected human colonic tissues first demonstrated that sEH expression was significantly up-regulated in UC-associated dysplasia and adenocarcinoma, but was minimally expressed in non-neoplastic colonic epithelia, mainly in the reactive hyperplastic epithelium. Our previous study showed *sEH* gene-deficiency attenuates inflammatory activity and tumor development in the bowel in spontaneous IBD in IL-10 knockout mice (11). In the present study, we further demonstrated that *sEH* gene-deficiency in DSS-induced colitis in mice led to the reduction of ulcerative inflammatory activity and induced tumor development in the colon. These findings indicate that sEH plays a crucial role in colitis-induced carcinogenesis.
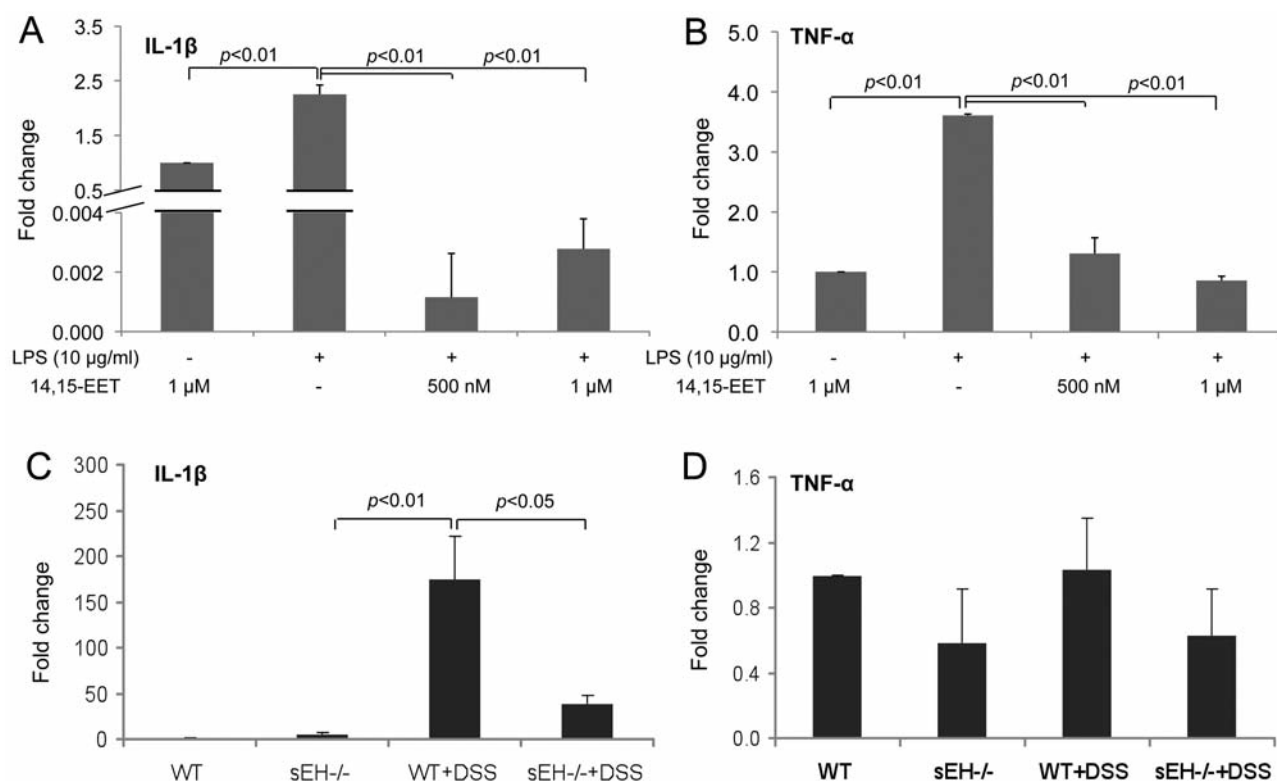
Figure 5. *Quantitative real time-RT-PCR analysis of expressions of inflammatory cytokines and chemokines. A significant decrease of mRNA expression of interleukin-1 beta (IL-1β) (A) and tumor necrosis factor alpha (TNF-α) (B) in macrophages isolated from peritoneal cavity treated with lipopolysaccharide (LPS) and 14,15-EET. A significant decrease of mRNA expression of IL-1β (C) and TNF-α (D) in freshly-collected colonic mucosa from sEH$^{-/-}$ mice as compared to wild-type (WT) mice (n=6 mice/group). Results are reported as the mean±SD. The statistically significant difference is labeled in the figure.*

Long-standing chronic active IBD is a high-risk factor for cancer development. Several key molecular events involved in chronic active inflammatory processes contribute to cancer development, including the overproduction of reactive oxygen and nitrogen species, aberrant metabolites of key arachidonic acid metabolism, overproduction of cytokines/chemokines, and the dysfunction of the immunity system (7). Inflammatory cells especially neutrophils and macrophages, play a central role in these molecular events (30). Targeting inflammatory cell infiltration would be a key event to suppress inflammatory activity and inflammation-induced carcinogenesis. Our study indicated that *sEH* gene-deficiency in mice led to a significant decrease of MPO-labeled active inflammatory cells in the inflamed colonic mucosa that paralleled the reduction of colonic tumor development. This further supports that inhibition of active inflammation leads to blocking of colitis-induced carcinogenesis.

The direct biological action of *sEH* gene-deficiency is to stabilize EETs *via* inactivation of the conversion of EETs to DHETs by sEH. Elevation of EETs prevents the amplification of several inflammatory events by inhibition of transcription factor NF-kB and IkappaB kinase (IkB),

including down-regulation of pro-inflammatory proteins, such as TNF-α, IL-1ß and iNOS, as well as VCAM1 and MCP1 (10). The cell adhesion molecule VCAM1 appears to be a key molecule for leukocyte adhesion to endothelial cells and infiltration into inflamed areas (14, 31-35). In the present study, using a powerful LC/MS-MS assay, we analyzed the effect of *sEH* gene-knockout on arachidonic acid metabolic profile and showed a significant increase of ratios of fatty epoxides-to-diols and EETs-to-DHETs, a biomarker for *sEH* gene-deficiency and inhibition. We further demonstrated that the expressions of TNFα, VCAM1, MCP1, IL-1ß, and iNOS were significantly reduced in sEH$^{-/-}$ mice with DSS-induced colitis. Further mechanistic study using *in vitro* LPS-activated macrophages demonstrated that treatment with EET significantly inhibited the expression of TNF-alpha and IL-1 beta in the active macrophages. All of these findings indicate that EETs play a central role in anti-inflammatory activity *via* targeting sEH.

In addition to stabilization of EETs, whether or not *sEH* gene-deficiency modulates other arachidonic metabolic pathways, such as COX and LOX metabolites, is an important question that needs to be fully addressed. Our
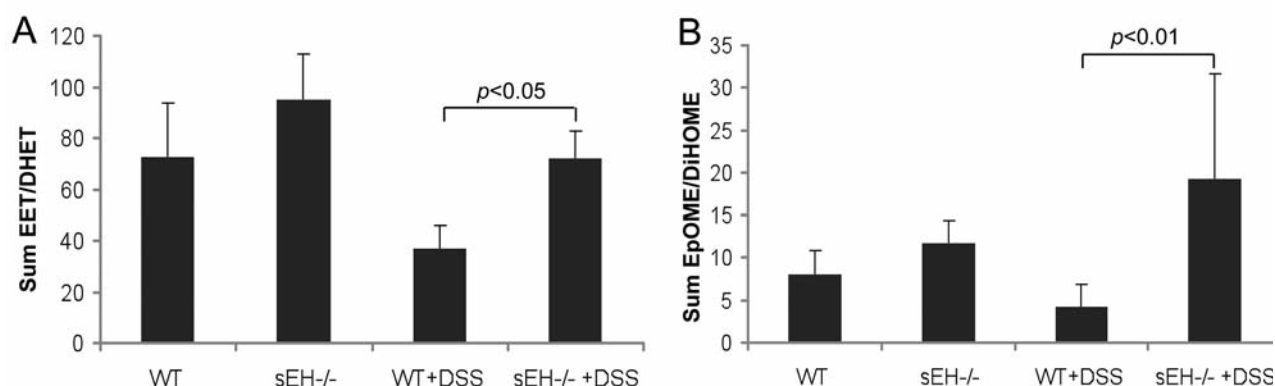
Figure 6. *Eicosanoid profile in plasma specimens analyzed using a liquid chromatographic/mass spectrometric (LC/MS-MS) method. The levels of epoxygenase-dependent metabolites in plasma expressed as the ratio of epoxyeicosatrienoic acids (EETs)-to-dihydroeicosatrienoic (DHETs) (A) and the ratio of total epoxyoctadecennoic acid (EpOME)-to-dihydroxyoctadecenoic acid (DiHOME) (B) are shown. Total EETs include 9(10)-, 11(12), and 14(15)-EET and total DHETs include 9(10)-, 11(12), and 14(15)-DHET. Total EpOMEs include 9(10)- and 11(12)-EpOME and total DHETs include 9(10)- and 11(12)-DiHOME. Results are reported as the mean±SD. The statistically significant difference is labeled in the figure.*

previous study demonstrated that sEH deficiency in spontaneous colitis in IL-10-knockout mice leads to mild modulation of LOX and COX-mediated metabolites, including minimal increase of LTB4 and 5-HETE, and mild decrease of PGE2, indicating potential feedback regulation on arachidonic acid metabolism (11, 14). Schmelzer *et al*. reported that although inhibition of sEH with 12-(3-adamantane-1-yl-ureido)-dodecanoic acid *n*-butyl ester (AUDA-nBE) does not directly inhibit phospholipase A_2, COX_2, TXB_2, or human 15-LOX1, it indirectly altered the production of LPS-induced COX and LOX metabolites, reducing levels of PGD_2, PGE_2, TXB_2, 6-keto-PGF1α, and 5-HETE (35, 36). In the present study, using a LC/MS-MS approach, COX and LOX-mediated metabolites, including PGE_2, PGD_2, TXB_2, LTB_4 and 5-HETE, were analyzed and showed no significant difference between wild-type and $sEH^{-/-}$ mice. These differences may be due to either different inflammatory disease models, or there is an alternative pathway involved in long-term mild active chronic inflammation in the colon in *sEH*-knockout mice. Further study on analysis of the expression and activities of key enzymes involved in arachidonic acid metabolism is needed.

There is a concern that sEH inhibition may affect angiogenesis and cancer metastasis (37). In addition to anti-inflammatory action and regulating vascular tone, EETs modulate several signaling cascades and affect cell proliferation, cell migration and angiogenesis (9). Angiogenesis is an important pathophysiological process for wound healing and tissue regeneration, but it is also a crucial event involved in tumor progression and metastasis. The effect of EETs and sEH inhibition on either enhancing or blocking angiogenesis is critical (38-40). Our previous studies together with the present results showed that sEH gene deficiency attenuated inflammatory activity, reduced ulcer formation and tumor development in colitis models in mice, and there is no metastasis identified in these models of colitis (11, 14). These findings indicate that inhibition of inflammation *via* targeting sEH appears to be an important step for prevention of inflammation-induced cancer development.

In summary, over expression of sEH was first identified in human UC-associated dysplasia and adenocarcinoma. Using DSS-induced ulcerative colitis in mice, *sEH*-knockout in mice significantly reduced inflammatory activity and cancer development in the colon. Mechanistically, an increase of EETs and down-regulation of cytokines and chemokines play a crucial role in the inhibition of inflammatory activity and reduction of inflammatory cell infiltration and inflammation-induced carcinogenesis. These findings imply that sEH is an important target for inflammation and provide a strong foundation for the development of anti-inflammatory therapeutics as well as cancer prevention.

Acknowledgements

References

1 Maloy KJ: The Interleukin-23/interleukin-17 axis in intestinal inflammation. J Intern Med *263(6)*: 584-590, 2008.
2 Coussens LM and Werb Z: Inflammation and cancer. Nature *420(6917)*: 860-867, 2002.

3 Gupta RB, Harpaz N, Itzkowitz S, Hossain S, Matula S, Kornbluth A, Bodian C, and Ullman T: Histologic inflammation is a risk factor for progression to colorectal neoplasia in ulcerative colitis: a cohort study. Gastroenterology *133(4)*: 1099-1105, 2007.

4 Rutter M, Saunders B, Wilkinson K, Rumbles S, Schofield G, Kamm M, Williams C, Price A, Talbot I, and Forbes A: Severity of inflammation is a risk factor for colorectal neoplasia in ulcerative colitis. Gastroenterology *126(2)*: 451-459, 2004.

5 Chen Z, Laurence A, Kanno Y, Pacher-Zavisin M, Zhu BM, Tato C, Yoshimura A, Hennighausen L and O'Shea JJ: Selective regulatory function of Socs3 in the formation of IL-17-secreting T cells. Proc Natl Acad Sci USA *103(21)*: 8137-8142, 2006.

6 Jess T, Rungoe C, and Peyrin-Biroulet L: Risk of colorectal cancer in patients with ulcerative colitis: a meta-analysis of population-based cohort studies. Clin Gastroenterol Hepatol *10(6)*: 639-645, 2012.

7 Vidailhet M: Omega 3: is there a situation of deficiency in young children?. Arch Pediatr *14(1)*: 116-123, 2007.

8 Schaad NC, Magistretti PJ and Schorderet M: Prostanoids and their role in cell–cell interactions in the central nervous system. Neurochem Int *18(3)*: 303-322, 1991.

9 Morisseau C and Hammock BD: Impact of Soluble Epoxide Hydrolase and Epoxyeicosanoids on Human Health. Annu Rev Pharmacol Toxicol *53*: 37-58, 2013.

10 Norwood S, Liao J, Hammock BD and Yang GY: Epoxyeicosatrienoic acids and soluble epoxide hydrolase: potential therapeutic targets for inflammation and its induced carcinogenesis. Am J Transl Res *2(4)*: 447-457, 2010.

11 Zhang W, Liao J, Li H, Dong H, Bai H, Yang A, Hammock BD and Yang GY: Reduction of inflammatory bowel disease-induced tumor development in IL-10 knockout mice with soluble epoxide hydrolase gene deficiency. Mol Carcinog *52(9)*: 726-38, 2013.

12 Morisseau C, Newman JW, Tsai HJ, Baecker PA and Hammock BD: Peptidyl-urea based inhibitors of soluble epoxide hydrolases. Bioorg Med Chem Lett *16(20)*: 5439-5444, 2006.

13 Newman JW, Morisseau C, Harris TR and Hammock BD: The soluble epoxide hydrolase encoded by EPXH2 is a bifunctional enzyme with novel lipid phosphate phosphatase activity. Proc Natl Acad Sci USA *100(4)*: 1558-1563, 2003.

14 Zhang W, Yang AL, Liao J, Li H, Dong H, Chung YT, Bai H, Matkowskyj KA, Hammock BD and Yang GY: Soluble Epoxide Hydrolase Gene Deficiency or Inhibition Attenuates Chronic Active Inflammatory Bowel Disease in IL-10(–/–) Mice. Dig Dis Sci *57(10)*: 2580-2591, 2012.

15 Coskun M, Olsen AK, Holm TL, Kvist PH, Nielsen OH, Riis LB, Olsen J and Troelsen JT: TNF-alpha-induced down-regulation of CDX2 suppresses MEP1A expression in colitis. Biochim Biophys Acta *1822(6)*: 843-851, 2012.

16 Hokari R, Kurihara C, Nagata N, Aritake K, Okada Y, Watanabe C, Komoto S, Nakamura M, Kawaguchi A and Nagao S: Increased expression of lipocalin-type-prostaglandin D synthase in ulcerative colitis and exacerbating role in murine colitis. Am J Physiol Gastrointest Liver Physiol *300(3)*: G401-408, 2011.

17 Tuin A, Poelstra K, de Jager-Krikken A, Bok L, Raaben W, Velders MP and Dijkstra G: Role of alkaline phosphatase in colitis in man and rats. Gut *58(3)*: 379-387, 2009.

18 Liao J, Seril DN, Yang AL, Lu GG and Yang GY: Inhibition of chronic ulcerative colitis associated adenocarcinoma development in mice by inositol compounds. Carcinogenesis *28(2)*: 446-454, 2007.

19 Popivanova BK, Kitamura K, Wu Y, Kondo T, Kagaya T, Kaneko S, Oshima M, Fujii C and Mukaida N: Blocking TNF-alpha in mice reduces colorectal carcinogenesis associated with chronic colitis. J Clin Invest *118(2)*: 560-570, 2008.

20 Seril DN, Liao J, Ho KL, Warsi A, Yang CS and Yang GY: Dietary iron supplementation enhances DSS-induced colitis and associated colorectal carcinoma development in mice. Dig Dis Sci *47(6)*: 1266-1278, 2002.

21 Seril DN, Liao J, Ho KL, Yang CS and Yang GY: Inhibition of chronic ulcerative colitis-associated colorectal adenocarcinoma development in a murine model by N-acetylcysteine. Carcinogenesis *23(6)*: 993-1001, 2002.

22 Seril DN, Liao J and Yang GY: Colorectal carcinoma development in inducible nitric oxide synthase-deficient mice with dextran sulfate sodium-induced ulcerative colitis. Mol Carcinog *46(5)*: 341-353, 2007.

23 Talero E, Sanchez-Fidalgo S, Villegas I, de la Lastra CA, Illanes M and Motilva V: Role of different inflammatory and tumor biomarkers in the development of ulcerative colitis-associated carcinogenesis. Inflamm Bowel Dis *17(3)*: 696-710, 2011.

24 Sanchez-Fidalgo S, Villegas I, Cardeno A, Talero E, Sanchez-Hidalgo M, Motilva V and Alarcon de la Lastra C: Extra-virgin olive oil-enriched diet modulates DSS-colitis-associated colon carcinogenesis in mice. Clin Nutr *29(5)*: 663-673, 2010.

25 Luria A, Weldon SM, Kabcenell AK, Ingraham RH, Matera D, Jiang H, Gill R, Morisseau C, Newman JW and Hammock BD: Compensatory mechanism for homeostatic blood pressure regulation in Ephx2 gene-disrupted mice. J Biol Chem *282(5)*: 2891-2898, 2007.

26 Enayetallah AE, French RA, Barber M and Grant DF: Cell-specific subcellular localization of soluble epoxide hydrolase in human tissues. J Histochem Cytochem 54(3): 329-335, 2006.

27 Enayetallah AE, French RA and Grant DF: Distribution of soluble epoxide hydrolase, cytochrome P450 2C8, 2C9 and 2J2 in human malignant neoplasms. J Mol Histol *37(3-4)*: 133-141, 2006.

28 Roques M, Bagrel D, Magdalou J and Siest G: Expression of arylhydrocarbon hydroxylase, epoxide hydrolases, glutathione S-transferase and UDP-glucuronosyltransferases in H5-6 hepatoma cells. Gen Pharmacol *22(4)*: 677-684, 1991.

29 Yang MD, Wu CC, Chiou SH, Chiu CF, Lin TY, Chiang IP and Chow KC: Reduction of dihydrodiol dehydrogenase expression in resected hepatocellular carcinoma. Oncol Rep *10(2)*: 271-276, 2003.

30 Roncucci L, Mora E, Mariani F, Bursi S, Pezzi A, Rossi G, Pedroni M, Luppi D, Santoro L and Monni S: Myeloperoxidase-positive cell infiltration in colorectal carcinogenesis as indicator of colorectal cancer risk. Cancer Epidemiol Biomarkers Prev *17(9)*: 2291-2297, 2008.

31 Fleming I, Fisslthaler B, Dimmeler S, Kemp BE and Busse R: Phosphorylation of Thr(495) regulates Ca(2+)/calmodulin-dependent endothelial nitric oxide synthase activity. Circ Res *88(11)*: E68-75, 2001.

32 Liu JY, Yang J, Inceoglu B, Qiu H, Ulu A, Hwang SH, Chiamvimonvat N and Hammock BD: Inhibition of soluble epoxide hydrolase enhances the anti-inflammatory effects of aspirin and 5-lipoxygenase activation protein inhibitor in a murine model. Biochem Pharmacol *79(6)*: 880-887, 2010.

33 Manhiani M, Quigley JE, Knight SF, Tasoobshirazi S, Moore T, Brands MW, Hammock BD and Imig JD: Soluble epoxide hydrolase gene deletion attenuates renal injury and inflammation with DOCA-salt hypertension. Am J Physiol Renal Physiol *297(3)*: F740-748, 2009.

34 Node K, Huo Y, Ruan X, Yang B, Spiecker M, Ley K, Zeldin DC and Liao JK: Anti-inflammatory properties of cytochrome P450 epoxygenase-derived eicosanoids. Science *285(5431)*: 1276-1279, 1999.

35 Schmelzer KR, Kubala L, Newman JW, Kim IH, Eiserich JP and Hammock BD: Soluble epoxide hydrolase is a therapeutic target for acute inflammation. Proc Natl Acad Sci USA *102(28)*: 9772-9777, 2005.

36 Schmelzer KR, Inceoglu B, Kubala L, Kim IH, Jinks SL, Eiserich JP and Hammock BD: Enhancement of antinociception by coadministration of nonsteroidal anti-inflammatory drugs and soluble epoxide hydrolase inhibitors. Proc Natl Acad Sci USA *103(37)*: 13646-13651, 2006.

37 Panigrahy D, Edin ML, Lee CR, Huang S, Bielenberg DR, Butterfield CE, Barnes CM, Mammoto A, Mammoto T and Luria A: Epoxyeicosanoids stimulate multiorgan metastasis and tumor dormancy escape in mice. J Clin Invest *122(1)*: 178-191, 2012.

38 Cui PH, Petrovic N and Murray M: The omega-3 epoxide of eicosapentaenoic acid inhibits endothelial cell proliferation by p38 MAP kinase activation and cyclin D1/CDK4 down-regulation. Br J Pharmacol *162(5)*: 1143-1155, 2011.

39 Fleming I: The cytochrome P450 pathway in angiogenesis and endothelial cell biology. Cancer Metastasis Rev *30(3-4)*: 541-555, 2011.

40 Panigrahy D, Greene ER, Pozzi A, Wang DW and Zeldin DC: EET signaling in cancer. Cancer Metastasis Rev *30(3-4)*: 525-540, 2011.